

Chapter 21

The nonlinear response of Boolean models: elasticity and conductivity

FRANÇOIS WILLOT & DOMINIQUE JEULIN

Mines ParisTech, PSL – Research University, Centre for Mathematical Morphology, 35 rue Saint-Honoré, 77300 Fontainebleau, France

Keywords: Fourier methods; Boolean models; Nonlinear elasticity

Abstract The effective response of an ideal random composite, the Boolean model of spheres, with a nonlinear powerlaw matrix, is investigated. Nonlinearity is parametrized by the law exponent $0 \leq n \leq 1$, with the values $n = 1$ corresponding to a linear-elastic matrix and $n = 0$ to a strongly nonlinear elastic matrix. To strengthen the effect of the microstructure, inclusions are either quasi-rigid or porous, whereas the matrix is compressible or incompressible. Full-fields solutions are computed numerically using Fourier methods, for varying inclusion volume fractions and nonlinearity exponent. Next, we consider the effect of a two-scale dispersion of pores and rigid inclusions in the context of a nonlinear matrix.

21.1 Constitutive law and loading conditions

This work is concerned by the mechanical behavior of a Boolean model of porous or quasi-rigid spheres with volume fraction f embedded in a matrix. In the matrix, the stress tensor σ obeys the following “powerlaw” behavior:

$$\sigma_m(\mathbf{x}) = 3\kappa_m(\mathbf{x})\varepsilon_m(\mathbf{x}), \quad \sigma'(\mathbf{x}) = \frac{2y_m}{3\varepsilon_{\text{eq}}(\mathbf{x})^{1-n}}\varepsilon'(\mathbf{x}), \quad (21.1)$$

where σ' , ε' and ε_{eq} are the deviatoric stress and strain tensors and the Von Mises equivalent strain:

$$\begin{aligned} \sigma'_{ij} &= \sigma_{ij} - \sigma_m \delta_{ij}, & \varepsilon'_{ij} &= \varepsilon_{ij} - \varepsilon_m \delta_{ij}, & \varepsilon_m &= \varepsilon_{ii}/3, & \sigma_m &= \sigma_{ii}/3, \\ \varepsilon_{\text{eq}} &= \sqrt{(2/3)\varepsilon' : \varepsilon'}, & \sigma_{\text{eq}} &= \sqrt{(3/2)\sigma' : \sigma'}, \end{aligned} \quad (21.2)$$

and δ_{ij} is the Kronecker symbol. When $n = 0$, the tangent elastic moduli is zero whenever $\varepsilon_{\text{eq}} > 0$. This law mimics a rigid perfectly-plastic behavior with yield stress y_m , assuming no local unloading occurs. In particular, one has $\sigma_{\text{eq}} = y_m \varepsilon_{\text{eq}}^n$. In the matrix, we set $y_m = 1$, and $\kappa_m = 1/3$ (compressible material) or $\kappa_m = 1/3 \cdot 10^3$ (quasi-incompressible matrix). In the inclusions, we set $\sigma \equiv 0$ for pores. Quasi-rigid inclusions are linearly-elastic with bulk and shear moduli equal to $1/3 \cdot 10^3$

The nonlinear conducting behavior in the matrix reads:

$$J_i(\mathbf{x}) = \chi_m |\mathbf{E}(\mathbf{x})|^{n-1} E_i(\mathbf{x}), \quad (21.3)$$

where \mathbf{J} is the current field, \mathbf{E} the electric field and where the nonlinear susceptibility χ_m is equal to 1. In insulating inclusions, we set $\mathbf{J} \equiv 0$, and, in highly-conducting inclusions, $\mathbf{J} = \chi_i \mathbf{E}$ with $\chi_i = 10^3$.

In elasticity, the equilibrium problem with periodic boundary conditions is solved using a FFT-based scheme (Michel, Moulinec, and Suquet 2000). The conductivity problem is solved using the same augmented-Lagrangian technique, applied to conductivity (Michel, Moulinec, and Suquet 2001). To achieve convergence, the constitutive law (21.1), which presents an infinite slope at the origin when $n \neq 1$, is regularized as follows. For elasticity we introduce a linear-elastic regime and enforce:

$$\sigma_{\text{eq}} = \min(3\mu\varepsilon_{\text{eq}}, y_m\varepsilon_{\text{eq}}^n),$$

with $\mu = 10^3 \gg 1$. Thus, the second equation in (21.1) is replaced by:

$$\sigma' = \min\left(2\mu, \frac{2y_m}{3\varepsilon_{\text{eq}}(\mathbf{x})^{1-n}}\right) \varepsilon'(\mathbf{x}),$$

Likewise, we set, in the conductivity problem:

$$\mathbf{J} = \min(\chi_1|\mathbf{E}|, \chi_m|\mathbf{E}|^n) \frac{\mathbf{E}}{|\mathbf{E}|},$$

where $\chi_1 = 10^3$.

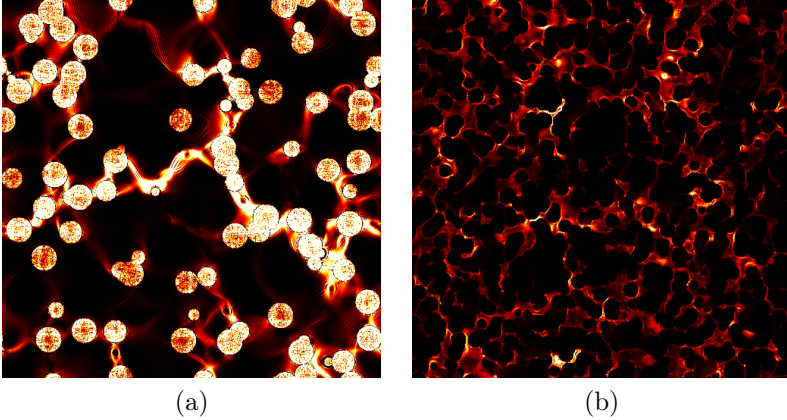


Figure 21.1: FFT maps: 2D section of the Von Mises equivalent deviatoric strain ε_{eq} . (a) strongly nonlinear matrix with porous inclusions of volume fraction $f = 5\%$ (b) strongly nonlinear matrix with quasi-rigid inclusions of volume fraction $f = 60\%$. Hydrostatic strain loading $\langle \varepsilon_m \rangle > 0$ is applied. Highest strain values in yellow and white, lowest in black. The matrix is incompressible in (a), and compressible in (b).

In the following we apply two types of strain loading conditions, of the form $\langle \varepsilon_{ij} \rangle = t \bar{\varepsilon}_{ij}$ where $t = 1$ is a loading parameter and $\bar{\varepsilon}_{ij}$ is the loading direction (here $\langle \cdot \rangle$ denotes a spatial average). The first loading type is a hydrostatic strain loading $\bar{\varepsilon}_{ij} = \delta_{ij}$. We define the effective “bulk modulus” κ_0 by the relation:

$$\kappa_0 = \langle \sigma_m \rangle / (3 \langle \varepsilon_m \rangle^n), \quad (21.4)$$

with $\langle \varepsilon_m \rangle = 1$ in the computations carried out in the present work. The second loading condition is a shear strain loading $\bar{\varepsilon}_{12} = \bar{\varepsilon}_{21} = 1$ with the other strain components equal to zero. The effective yield stress y_0 is defined by:

$$\langle \sigma \rangle_{\text{eq}} = y_0 \langle \varepsilon \rangle_{\text{eq}}^n, \quad (21.5)$$

In conductivity, we apply a macroscopic applied electric field $\langle E_x \rangle = 1$ and define the effective susceptibility χ_0 by:

$$|\langle \mathbf{J} \rangle| = \chi_0 |\langle \mathbf{E} \rangle|^n. \quad (21.6)$$

21.2 FFT results

21.2.1 Boolean microstructure

In the numerical computations that follow, we discretize the Boolean model of spheres over regular grids of points of volume 512^3 voxels. The spheres diameter is 20 voxels and the intensity of the Poisson point process in the Boolean model is chosen so as to guarantee, on average, a sphere volume fraction equal to f . Examples of field maps for a strongly nonlinear matrix ($n = 0$) are shown in Fig. (21.1).

FFT results for the effective bulk modulus and yield stress of a rigidly-reinforced Boolean model of spheres are shown in Fig. (21.2) as a function of the volume fraction of rigid particles, for various exponents n . The effective bulk modulus decreases when the nonlinearity increases. This effect is weak for small density of spheres and more pronounced after the percolation threshold, when the density of rigid particles typically lies in the range $[0.7; 0.9]$, highlighting a strong effect of nonlinearity in this regime.

In the semi-log scale representation of Fig. (21.2b), this situation appears to be reversed for the yield stress, which is sensitive to the nonlinearity exponent when the density of spheres is less than about 0.4 and low afterwards. In contrast to the data presented for the bulk modulus, the effective yield stress presents, in the dilute limit, a slope (first-order correction) which vary with n . More precisely, the correction decreases with n , and approaches a zero-slope when n goes to 0, i.e. a weak effect of rigid particles when $n = 0$. Limit analysis predicts that the effective yield stress y_0 equals y_m if there exists a planar surface entirely contained in the matrix. In periodic media, this leads to $y_0 = y_m$ in a large domain (Idiart et al. 2009). This is not the case in random media, where such surfaces do not exist.

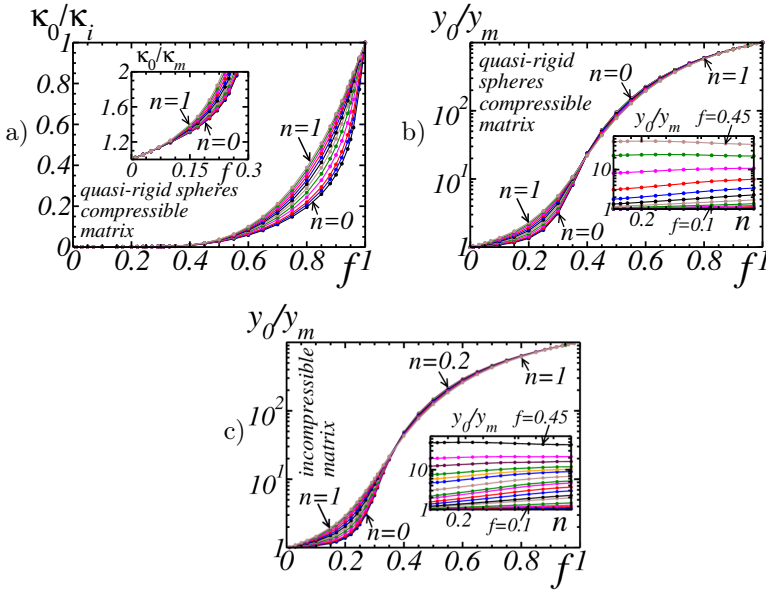


Figure 21.2: Normalized effective bulk modulus κ_0/κ_i (a) and normalized yield stress σ_0/y_m (b-c) for a Boolean model of quasi-rigid spheres of volume fraction f , for varying powerlaw exponent $n = 0, \dots, 1$ in the matrix. The matrix is compressible with bulk modulus $\kappa_m = 1$ (a-b) or quasi-incompressible ($\kappa_m = 10^3$) (c).

In the porous case, the effective yield stress is quite insensitive to the nonlinearity exponent (Fig. 21.3c, 21.3d). The effective bulk modulus however is much weaker for strongly nonlinear matrices than with a linear matrix. This sensitivity is exacerbated

when the matrix is incompressible (Fig. 21.3b).

Results obtained for conductivity are shown in Fig. (21.4). The effective conductivity is not a monotonic function of n at fixed f . In the insulating case, it takes its maximum value at about $n \approx 0.7$ for most sphere volume fraction.

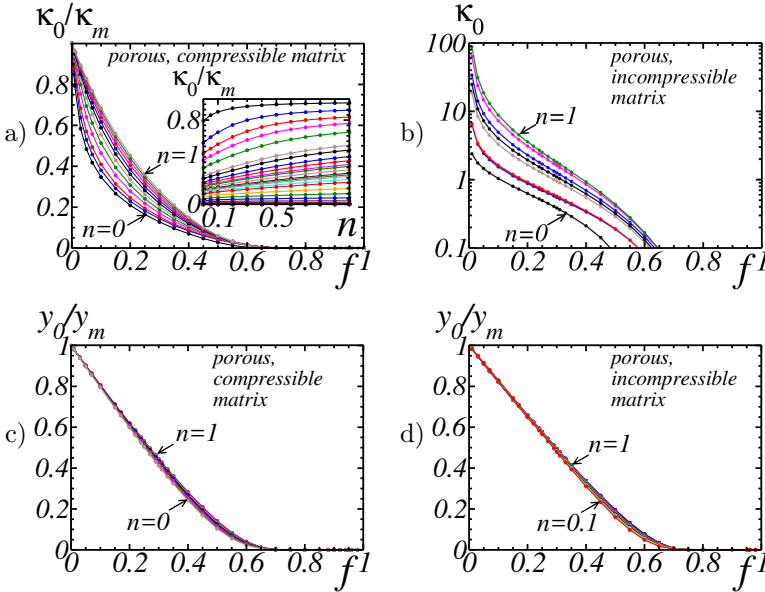


Figure 21.3: Effective bulk modulus κ_0 (a-b) and yield stress y_0 (c-d) of a Boolean model of porous spheres as a function of the sphere volume fraction f , for varying powerlaw exponent $n = 0, \dots, 1$ in the matrix. (a), (c): Compressible matrix. (b), (d): Quasi-incompressible matrix.

21.2.2 Two-scale microstructures

Consider a Cox-Boolean model made of aggregates of spheres, as introduced in another study (Willot and Jeulin 2011). This model is simulated using (i) a Boolean model of spheres of large radius and (ii) a Boolean model of spheres with smaller radius which lie inside the larger spheres. We assume that the volume fraction of the largest spheres in the whole domain is equal to the volume fraction of the small spheres relative to the larger spheres. After this process, we keep the small spheres only. Assuming scale separation between the smallest and largest spheres, this two-scales material depends on one parameter only, the sphere volume fraction, like the homogeneous Boolean model. However, contrary to the one-scale model, the spheres in the Cox-Boolean model are aggregated into clusters, whose size is parametrized by the radius of the largest spheres. In the numerical computations that follow, we discretize the smallest and largest spheres using diameters of 5 and 50 voxels, and the two-scales Boolean model are discretized on grids of 512^3 voxels as before. For simplicity, only the strongly nonlinear ($n = 0$) and linear regimes ($n = 1$) are considered.

In a previous study (Willot and Jeulin 2011) devoted to the linear-elastic regime, it has been shown that the non-uniform dispersion of spheres greatly increases the elastic properties at fixed volume fraction of inclusions, when rigid inclusions are considered. The corresponding results in the nonlinear regime are shown in Fig. (21.5b). For strongly nonlinear matrices ($n = 0$) a reinforcement effect due to the non-uniform spatial dispersion is also observed, when $f < 0.3$. This is not so at higher rigid-inclusions volume

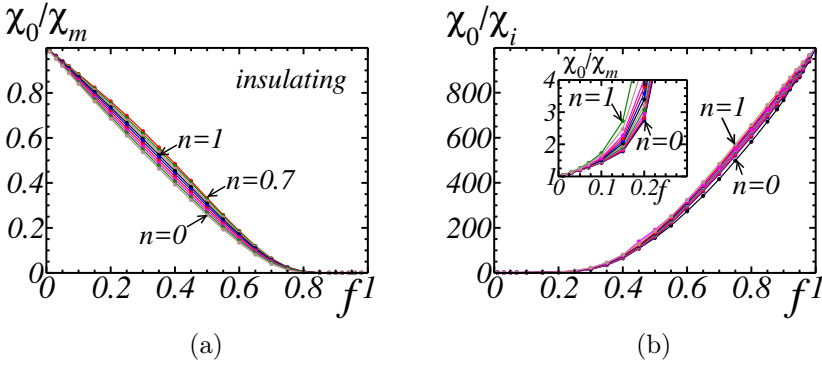


Figure 21.4: Normalized effective conductivity χ_0/χ_m and χ_0/χ_i of a Boolean model of highly-conducting (a) and insulating (b) spheres, as a function of the sphere volume fraction f , for varying powerlaw exponent $n = 0, \dots, 1$ in the matrix.

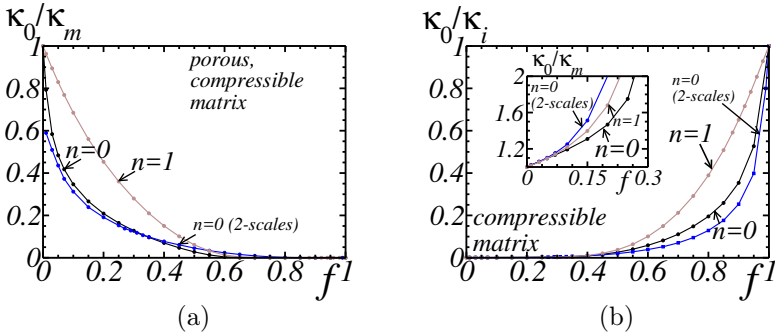


Figure 21.5: Effective bulk modulus κ_0 in the one-scale and “iterated” two-scales porous and rigidly-reinforced Boolean models, as a function of the sphere volume fraction f , at varying powerlaw exponent $n = 0, \dots, 1$ in the matrix.

fractions. In contrast to the linear case, our data suggests a weakening effect of the non-uniform dispersion.

The study mentioned previously (Willot and Jeulin 2011) has shown that, in the linear regime, pores have a stronger effect when they are aggregated into clusters. This property holds in for strongly nonlinear matrices ($n = 0$) when $f \leq 0.3$ Fig. (21.5a). The weakening of the macroscopic behavior due to a non-uniform dispersion of pores has been observed previously, e.g. in (Bilger et al. 2005). When $f \geq 0.3$, however, the effective bulk modulus for the one-scale model is lower than that in the two scales model (Fig. 21.5a).

21.3 Conclusion

The reinforcement and weakening effect of a population of pores or quasi-rigid inclusions has been estimated numerically, in the context of a matrix with powerlaw nonlinear response. Nonlinearity has an important weakening effect on the effective bulk modulus in rigidly-reinforced media with particles volume fraction beyond the percolation threshold. However, the most dramatic effect of nonlinearity is observed in porous media with quasi-incompressible matrix, and for small volume fraction of pores. This is in contrast with results obtained for the effective yield stress which is, in porous media, weakly-sensitive to the nonlinearity exponent, except possibly in the dilute regime.

Computations have also been carried out on a two-scale Cox-Boolean material with non-uniform particles dispersion. In the linear regime, a reinforcement effect of the two-scale dispersion is observed in the rigid case. This property does not hold for strongly nonlinear matrices with exponent $n = 0$, in particular at high volume fractions of rigid particles.

References

- Bilger, Nicolas, François Auslender, Michel Bornert, Jean-Claude Michel, Hervé Moulinec, Pierre Suquet, and André Zaoui (2005). “Effect of a nonuniform distribution of voids on the plastic response of voided materials: a computational and statistical analysis”. In: *International Journal of Solids and Structures* 42.2, pp. 517–538.
- Idiart, M.I., F. Willot, Y.-P. Pellegrini, and P. Ponte Castaneda (2009). “Infinite-contrast periodic composites with strongly nonlinear behavior: effective-medium theory versus full-field simulations”. In: *International Journal of Solids and Structures* 46.18, pp. 3365–3382.
- Michel, J.-C., H. Moulinec, and P. Suquet (2000). “A computational method based on Augmented Lagrangians and Fast Fourier Transforms for composites with high contrast”. In: *Computer Modelling in Engineering & Sciences* 1.2, pp. 79–88.
- (2001). “A computational scheme for linear and non-linear composites with arbitrary phase contrast”. In: *International Journal for Numerical Methods in Engineering* 52.1–2, pp. 139–160.
- Willot, F. and D. Jeulin (2011). “Elastic and electrical behavior of some random multiscale highly-contrasted composites”. In: *International Journal for Multiscale Computational Engineering: special issue on Multiscale modeling and uncertainty quantification of heterogeneous materials* 9.3, pp. 305–326.